Molecular Cell *23*, 523–533, August 18, 2006 ©2006 Elsevier Inc. DOI 10.1016/j.molcel.2006.06.020

Engineered Hybrid Dimers: Tracking the Activation Pathway of Caspase-7

Jean-Bernard Denault,[1] Miklós Békés,[1] Fiona L. Scott,[1] Kelly M.B. Sexton,[2] Matthew Bogyo,[2,3] and Guy S. Salvesen[1,*]
[1]The Burnham Institute for Medical Research
10901 North Torrey Pines Road
La Jolla, California 92037
[2]Department of Pathology
[3]Department of Microbiology and Immunology
Stanford University School of Medicine
300 Pasteur Drive
Stanford, California 94305

Summary

Caspase-7 is an obligate dimer of catalytic domains, with generation of activity requiring limited proteolysis within a region that separates the large and small chains of each domain. Using hybrid dimers we distinguish the relative contribution of each domain to catalysis by the whole molecule. We demonstrate that the zymogen arises from direct dimerization and not domain swapping. In contrast to previous conclusions, we show that only one of the catalytic domains must be proteolyzed to enable activation. The processed domain of this singly cleaved zymogen has the same catalytic activity as a domain of fully active caspase-7. A transient intermediate of singly cleaved dimeric caspase-7 can be found in a cell-free model of apoptosis induction. However, we see no evidence for an analogous intermediate of the related executioner caspase-3. Our study demonstrates the efficiency by which the executioner caspases are activated in vivo.

Introduction

Caspases constitute a family of cytosolic proteases with a stringent specificity for cleaving target proteins after aspartate residue. They are synthesized as zymogens awaiting activation by one of the routes available within a cell. During apoptosis in humans, initiator caspase-8, -9 and/or -10, which integrate molecular signals into proteolytic activity, are activated by dimerization at the death-inducing signaling complex (DISC, caspase-8 and -10) or the apoptosome (caspase-9). Once activated, the initiators activate the executioner zymogens by direct limited proteolysis, thus amplifying the apoptotic signal (Boatright and Salvesen, 2003). Activated executioner caspases cleave a limited set of cellular substrates (Fischer et al., 2003), thereby causing the demise of the cell through a set of hallmarks (Green and Evan, 2002).

Cleavage in a region between the large and small subunits (or chains), called the interchain connector, is the only requirement of executioner caspases to gain full activity. Whereas the site of cleavage within the connector may not directly impact the activity of the caspase (Zhou and Salvesen, 1997), it has important repercussions for its regulation. Cleavage of caspases reveals a new N terminus that often facilitates caspase inhibition by endogenous regulators (Riedl and Shi, 2004; Scott et al., 2005).

The zymogens of the executioner caspase-3 and -7 are homodimers, and therefore, they contain two potential active sites and two interchain connectors per molecule. A molecule of procaspase-3 originates from the association of two monomeric folding intermediates, and the domains are tightly associated in the procaspase-3 dimer (Bose and Clark, 2001). It is likely that this holds for caspase-7, which from a structural and mechanistic point of view provides a better paradigm, because atomic resolution structures are available in the uncleaved zymogen form, the cleaved, unliganded form, and the cleaved, ligand bound form (Wei et al., 2000; Chai et al., 2001; Riedl et al., 2001). Together, these structures reveal that activation requires the movement of three surface loops that contain crucial elements of the catalytic apparatus and specificity sites. It is considered that cleavage in the interchain connectors has two essential functions: (1) removal of blocking segments that prevent translocation of one of these loops in the zymogen form and (2) allowing interactions between the newly formed terminals of the small and large chains from neighboring domains to stabilize the active conformation by forming a loop bundle with each other.

The prevailing view is that both interchain connectors must be cleaved to allow formation of an active enzyme, because both connectors must be removed from the central cavity at the dimer interface, with subsequent formation of the loop bundle (Chai et al., 2001; Riedl et al., 2001). Moreover, the active initiator caspases-8 and -10 are dimeric enzymes with active sites that can be docked, at least in silico, onto the general space occupied by the interchain connector region of procaspase-7, leading to the hypothesis that a concerted and cooperative mechanism may account for simultaneous cleavage of both connectors of the zymogen. The available crystal structures cannot answer these fundamental hypotheses, primarily because the interchain connector is an intrinsically mobile loop. Therefore, we tested the importance of the hypothesis that both interchain connectors in a procaspase-7 molecule must be cleaved to become active by a combination of kinetics, mutagenesis, and selecting engineered caspase-7 hybrids. We also tested the two competing models for the formation of executioner caspase zymogens: a domain swapping model (Pop et al., 2001; Roy et al., 2001; Wei et al., 2000; Wilson et al., 1994) and a direct dimerization model (Bose and Clark, 2001; Denault and Salvesen, 2002; Pop et al., 2001).

Results

Activation of Recombinant Caspase-7 by Initiator Caspases

Upon expression in *E. coli*, single chain procaspase-7 is converted to a large and a small chain by cleavage in the interchain connector, with a $>10^4$-fold increase in catalysis (Zhou and Salvesen, 1997). The connector contains

*Correspondence: gsalvesen@burnham.org

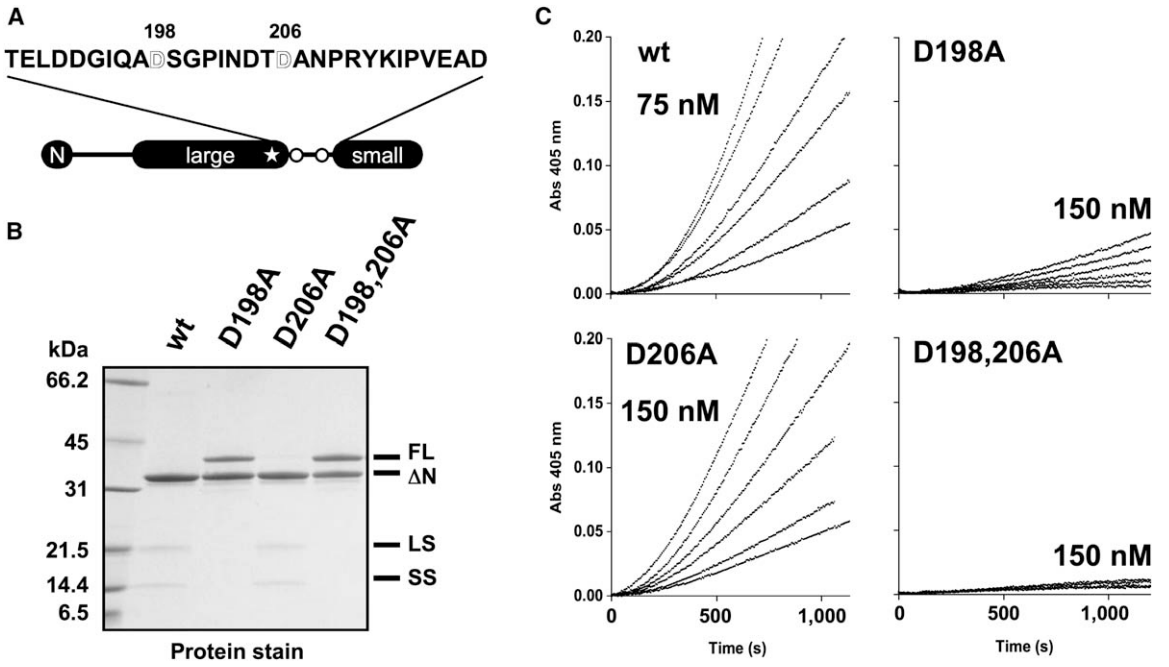

Figure 1. Kinetics of Procaspase-7 Activation by Initiator Caspases Show Strong Preference for Asp198

(A) Schematic representation of caspase-7 with the catalytic cysteine residue (star) and the two activation sites (open circles, outlined residues) found in its interchain connector. The "N" refers to the 23 amino acid N peptide removed during apoptosis and *E. coli* expression.

(B) The protein stain shows the integrity of the proteins used. Caspase-7 proteins carrying the D198A mutation are unable to activate efficiently and are less effective in processing the N peptide.

(C) Various concentrations of recombinant procaspase-7 activation site mutants were incubated with recombinant caspase-8 (25 nM) in the presence of 400 μM AcDEVD-pNA chromogenic substrate. A sample containing caspase-8 alone was used to determine its contribution to the hydrolysis of the substrate (<5%) and was subtracted to generate the datasets presented here. Similar experiments were carried out with caspase-2, -9, -10, and caspase-8:FLIP heterodimer. Activation rates were determined as described in the Experimental Procedures and are presented in Table 1. Procaspase-7 concentrations were as follows: wt: 75, 56, 42, 32, 24, and 18 nM; D198A: 150, 75, 56, 42, 32, and 24 nM; D206A: 150, 67, 44, 30, 20, and 13 nM; and D198A,D206A: 150, 75, 56, and 42 nM. The highest concentration of procaspase-7 is indicated for each panel. ΔN, full-length protein lacking the N peptide; FL, full-length; and LS or SS, large or small subunit.

two aspartate residues that could serve as proteolytic activation sites for apical caspases-2, -8, -9, and -10 (Figure 1A). It is unclear which of the sites are preferred by apical caspases, and to determine this, we mutated each site separately, purified recombinant proenzymes (Figure 1B), and determined the kinetics of activation (Figure 1C and Table 1). For comparison of apical caspase activation of procaspase-7, we employed high-salt buffer, where initiator caspase-8, -9, and -10 are maximally active (Boatright et al., 2004). Under this condition, procaspase-7 was activated with k_{cat}/K_M values from 1.6 − 3.4 × 10^4/M/s, and mutagenesis indicates that the preferred site is Asp198 (Figure 1C and Table 1). Interestingly, each of the apical caspases showed only minor use of Asp206 as an activation site. There is a formal possibility that cleavage at Asp198 enhances processing at Asp206. We thus tested this possibility by processing at 198 with the natural caspase activator granzyme B (GrB), followed by processing at 206 by caspase-8 (see Figure S1 in the Supplemental Data available with this article online). Because further processing at Asp206 cannot be measured enzymatically and could contribute to the readout, we used the catalytic mutant of procaspase-7 and analyzed the result on SDS-PAGE. Differences in the generation of the small subunit cleaved at 206 (see Figure S1) were less than 4-fold, suggesting that cleavage at Asp206 is relatively independent of the status of cleavage at Asp198 for its accessibility to proteolysis by an initiator caspase. In contrast to the apical caspase-8, -9, and -10, caspase-2 was unable to efficiently activate wild-type (wt) caspase-7 (Table 1) at either site.

The zymogen of caspase-7 is a dimer and contains connectors from both catalytic units juxtaposed in the general area of the dimer interface (Chai et al., 2001; Riedl et al., 2001). This raises the intriguing possibility that both catalytic units of the dimeric procaspase-7 zymogen may be simultaneously processed at their respective Asp198 sites in a concerted cooperative manner. If true, one would expect a caspase-8 homodimer (two active sites) to be more than twice as effective as a caspase-8 heterodimer (one active site). Caspase-8 heterodimers were obtained by incubation in the presence of the inactive caspase-8 paralog FLIP (Boatright et al., 2004). Homo- and heterodimers were used in activation assays in which the same concentration of active caspase-8 active sites was employed. Activation rates were similar for homodimer and heterodimer (Table 1), pointing to the absence of detectable cooperativity.

Analysis of the crystal structures of cleaved caspases reveals a critical role for residue 291 (caspase-1 numbering; residue 192 in caspase-7) in the formation of a loop bundle that stabilize the active site (Chai et al., 2001). To test the importance of residue 192 in

Table 1. Activation Kinetics of Wt Caspase-7 and Activation Site Mutants

Activator	Caspase-7	k_{cat}/K_M (× 10^4/M/s)[a]	n/N[b]
	In High-Salt Caspase Buffer		
Caspase-8	Wt	1.6 ± 0.5	34/5
	D198A	0.2 ± 0.1	11/3
	D206A	1.3 ± 0.4	27/4
	D198A+D206A	0.32 ± 0.30	9/2
Caspase-9	Wt	3.4 ± 0.8	19/3
	D198A	0.08 ± 0.03	7/2
	D206A	1.4 ± 0.2	15/3
	D198A+D206A	0.07 ± 0.03	14/2
Caspase-10	Wt	1.7 ± 0.8	20/3
	D198A	0.05 ± 0.04	21/3
	D206A	1.2 ± 0.4	15/3
	D198A+D206A	0.025 ± 0.017	6/2
Caspase-2	Wt	0.05 ± 0.01	7/1
Caspase-8 (gf)[c]	Wt	2.9 ± 0.6	14/2
	D206A	2.6 ± 0.6	14/2
Caspase-8: FLIP (gf)[c]	Wt	2.0 ± 0.4	14/2
	D206A	2.4 ± 0.6	14/2
	In Standard Caspase Buffer		
Caspase-8	Wt	176 ± 66	21/3
Granzyme B	Wt	860[d]	–

[a] Values ± standard deviation are presented.
[b] "n" is the total number of datasets used to determined the activation rate; "N" is the number of independent series consisting of up to seven activation reactions. See the Experimental Procedures for criteria used to exclude datasets from final analysis.
[c] The values reported are for the number of active catalytic units not the molar amount of dimer. gf, gel filtration-purified proteins.
[d] Taken from Zhou and Salvesen (1997).

caspase-7, we expressed zymogens of radical and permissive mutants of caspase-7 Asp192, processed them with GrB, and measured their activity (Figure 2). Compared to wt caspase-7, the D192A mutant is marginally active (Figure 2B; see Table S1). Isosteric mutation to Asn (D192N) or with a residue of same charge (D192E) or with Gln (D192Q)—as found in caspase-8 and -10—did not restore comparable activity (Figure 2B; see Table S1). Because the contact between Asp192 and the cognate catalytic unit might be weakened by our mutations, we also determined the kinetic parameters in high-salt buffer, a condition that favors stability of caspases (Boatright et al., 2004). This helped to restore Michaelis-Menten behavior of the D192N and D192Q mutant but nowhere near the value obtained for wt caspase-7 (see Table S1). The critical role of Asp192 and surrounding residues is further supported by *E. coli* expression studies. Upon prolonged expression, caspase-7 large and small chains are further trimmed (see Figure S2B) with an accompanying decrease in catalytic activity and inability to bind the activity-based probe (ABP) biotinyl-VAD-fluoromethyl ketone (bVAD-FMK) (see Figure S2C). SDS-PAGE and mass spectrometry analysis of this preparation shows trimming of the large chain at Asp192 and the small chain at Asp206 (see Figure S2D). Because cleavage at Asp206 results in a fully active caspase (Scott et al., 2005), we conclude that excessive processing at Asp192 inactivates caspase-7.

We conclude that activation of procaspase-7 by apical caspases is a simple one-step process where Asp198 is the preferred cleavage site. We detect no cooperativity in the activation process, indicating that the two active sites of apical caspases are not functionally linked and that the dual active sites of an initiator caspase do not simultaneously engage the dual cleavage Asp198 sites in the caspase-7 zymogen.

Generation of Engineered Caspase-7 Dimer

The above kinetic analysis does not allow us to assess whether both interchain connectors in the caspase-7 zymogen dimer must be cleaved to activate the enzyme. To directly test this, we designed an expression system in which differentially tagged caspase-7 constructs are coexpressed in *E. coli*, spontaneously assembling to a heterodimer that we can select by serial affinity chromatography. As a proof of concept of this approach, we coexpressed a C-terminal His-tagged caspase-7

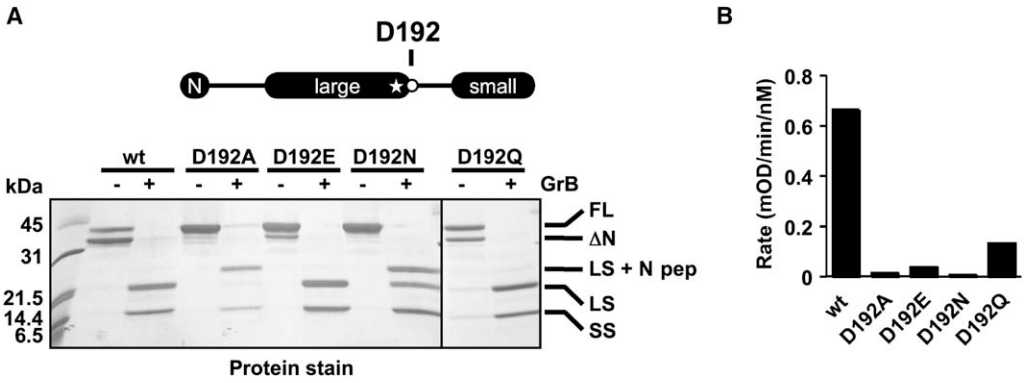

Figure 2. Aspartate 192 Is Critical for Caspase-7 Activity

(A) Granzyme B (GrB) processing of caspase-7 Asp192 mutants. Samples were left untreated or treated with GrB for 30 min, analyzed by SDS-PAGE, and stained with GelCode blue. Cleavage of more than 95% of the protein is routinely obtained showing that proteins are properly folded. Because caspase-7 removes its own N peptide, lack of N peptide removal equates to poor activity.

(B) Specific activity of GrB-processed caspase-7 Asp192 mutants was measured by using 200 μM AcDEVD-pNA chromogenic substrate and reported as a rate over protein concentration. The activity of every mutant was very low, but at least five times the background rate in assay buffer alone. Kinetic parameters for processed enzymes are reported in Table S1. ΔN, full-length protein lacking the N peptide; FL, full-length; LS or SS, large or small subunit; and N pep, N peptide.

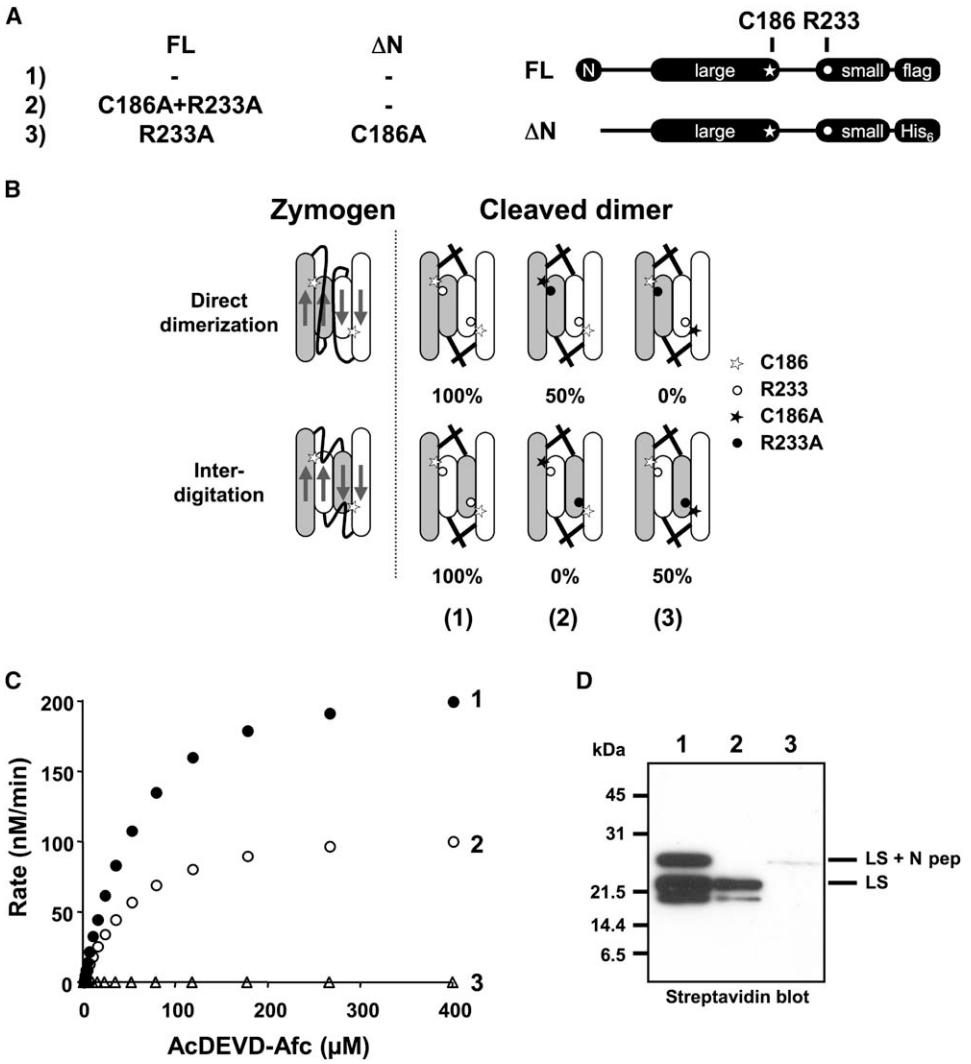

Figure 3. Caspase-7 Dimer Catalytic Units Do Not Form by Interdigitation

(A) Schematic representation of differentially tagged caspase-7 with the pertinent residue mutants.

(B) The three sets of possible heterodimers are described as pairs of caspase-7 proteins. Wt residues are shown as open symbols, and mutated ones as closed symbols. Due to complementation, the only active sites that can be formed are when two unmutated (open symbol) residues come together to generate catalytic activity. The theoretical activity generated for each model is shown.

(C) Equimolar amounts of GrB-processed dimers were incubated with a range of AcDEVD-AFC substrate concentrations, and initial rates were calculated. K_M and k_{cat} values are reported in Table S2. This result demonstrates that direct dimerization creates the caspase-7 dimer.

(D) GrB-processed caspase-7 dimers were incubated with 1 μM bVAD-FMK ABP for 30 min in assay buffer and analyzed with HRP-coupled streptavidin to detect the biotinylated active catalytic unit. LS or SS, large or small subunit; N pep, N peptide.

See Figure S4 for protein quantification and GrB cleavage.

and a C-terminally Flag-tagged caspase-7 (see Experimental Procedures). Each tagged protein can be distinguished on the basis of size because the N peptide of the His-tagged caspase-7 was made noncleavable by mutating the cleavage site Asp23 to Ala, whereas the Flag-tagged caspase-7 construct has the N peptide deleted (see Figure S3). This also allows for identification of which large subunit arises from which precursor: an approach made feasible because the N peptide has no influence on the enzymatic characteristics of caspase-7 in vitro (Denault and Salvesen, 2003). Coexpression of caspase-7 combinations lacking one of the affinity tags was used to demonstrate the specificity of the purification methods. Proteins were sequentially purified by immobilized metal affinity and anti-Flag adsorption (see Figure S3). It is only when both tags were present that caspase-7 was obtained, demonstrating that the purified protein is a dimer of differentially tagged catalytic domains. This hybrid enzyme can be active-site titrated and is enzymatically identical to recombinant purified His-tagged wt caspase-7 or untagged wt caspase-7 (see Figure S3 and Table S2).

Procaspase-7 Does Not Arise by Domain Swapping

Having developed a procedure to select caspase-7 heterodimers, we tested the domain swapping model for the formation of dimeric caspase zymogens (Roy et al., 2001; Wei et al., 2000; Wilson et al., 1994). This model (Figure 3B) is based on the close juxtaposition of the small chain N terminus and large chain C terminus

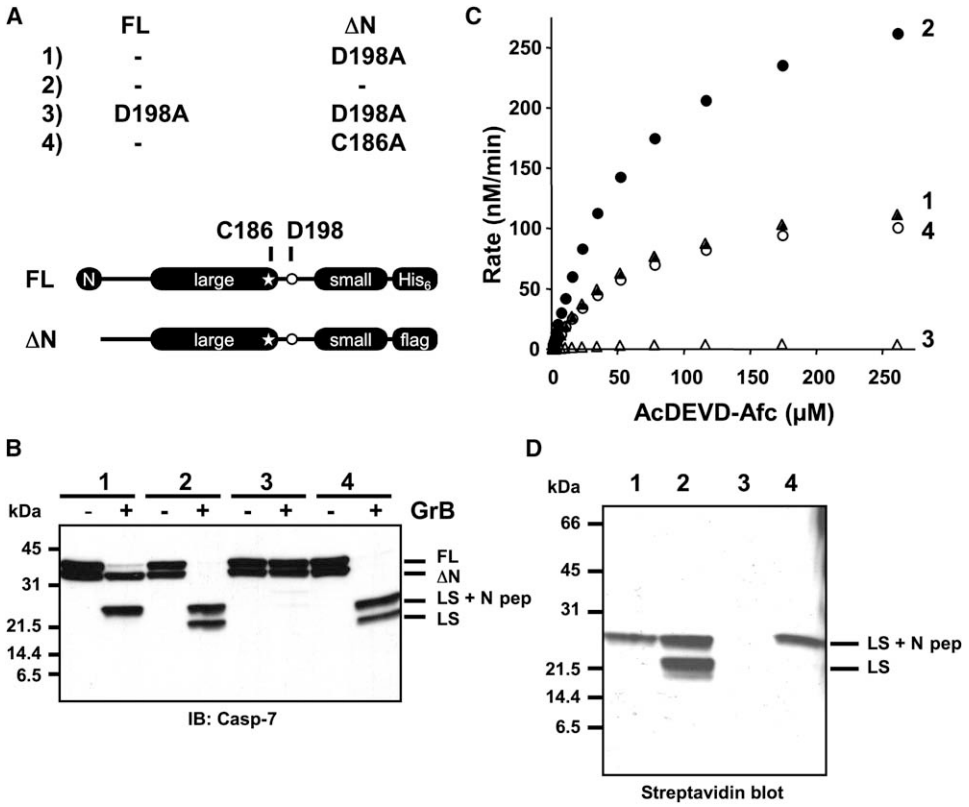

Figure 4. Caspase-7 Dimer with a Singly Cleaved Catalytic Unit Is Active

(A) Schematic representation of differentially tagged caspase-7 with the pertinent residue mutants. The four sets of heterodimers produced are described as pairs of caspase-7 proteins expressed.

(B) Samples were processed with GrB and analyzed by immunoblotting with a monoclonal caspase-7 antibody.

(C) Kinetic analysis of GrB-processed caspase-7 heterodimers was performed as in Figure 3C. Parameters are reported in Table S2.

(D) Active GrB-processed caspase-7 heterodimers catalytic units were labeled with bVAD-FMK as in Figure 3D. ΔN, full-length protein lacking the N peptide; FL, full-length; LS, large subunit; and N pep, N peptide.

See Figure S4 for protein expression and quantification.

observed in the structures of active caspases and was first proposed for caspase-1 (Wilson et al., 1994). The atomic resolution structures of neither the zymogen form of caspase-7 (Chai et al., 2001; Riedl et al., 2001) nor the several biochemical studies (Gu et al., 1995) have equivocated over the question. We selected heterodimers of procaspase-7 containing a C186A catalytic mutant and an R233A mutant in the primary specificity site (see Figure S4). Both mutations render caspase-7 inactive, but if the domain swapped model is correct, they should be able to complement each other if provided individually on the separate units of a dimer (Figure 3B). Dimers originating from single or doubly mutated procaspase-7 were purified and activated with GrB (Figures 3C and 3D). Kinetic analysis revealed that a dimer containing both mutations originating from the same catalytic unit displays half the activity of a wt dimer, whereas distributing mutations between catalytic units resulted in complete inactivation of the dimer (Figure 3C). This was confirmed when heterodimers were labeled with bVAD-FMK (Figure 3D). The results demonstrate that the formation of procaspase-7 by dimerization proceeds without domain swapping, which is consistent with conclusions reached from unfolding studies on the closely related executioner procaspase-3 (Bose and Clark, 2001).

Partially Processed Caspase-7 Dimer Is Active

To directly test the hypothesis that both catalytic units of a dimer must be cleaved to generate activity, we expressed and selected a hybrid dimer of caspase-7 containing one catalytic unit that had been mutated to prevent cleavage at Asp198. We extensively compared samples to each other by SDS-PAGE, several independent immunoblots (see Figure S4), and quantitative imaging (see Experimental Procedures). Purified proteins consisted of hybrid heterodimeric caspase-7 with less than 15% contamination with homodimer. Upon treatment with GrB, only the catalytic unit with an unmutated connector is processed, whereas the D198A mutation prevented cleavage (Figure 4B). Surprisingly, cleavage of one catalytic unit generated enzymatic activity similar to a fully processed dimer containing one inactive catalytic unit (C186A mutation) and about half the activity of a fully processed and active caspase-7 (Figure 4C). Kinetic analysis revealed that this singly processed caspase-7 is similar to wt enzyme (Figure 4C) in its affinity toward a fluorogenic substrate (K_M) but has about half the catalytic rate (k_{cat}) (see Table S2). The latter parameter would be entirely consistent with a dimer containing a single active catalytic unit.

Based on the hypothesis that cleavage of executioner caspases is the activating event, the simplest

interpretation of our result is that the activity obtained from the caspase-7 mutant heterodimer is from the cleaved catalytic unit. However, there is a formal possibility that activity arises within the uncleaved catalytic unit because the uncleaved activation loop is long enough to satisfy a competent catalytic site and preserve the contact made by Asp192 (see above) of the cleaved activation loop. To identify the active catalytic unit within this hybrid dimer, we incubated the processed proteins with bVAD-FMK and analyzed the samples for biotinylated protein with streptavidin-HRP (Figure 4D). In all cases, only the cleaved large subunit containing a functional catalytic cysteine was labeled with the ABP. Therefore, we conclude that a fully functional catalytic site is generated by cleavage of one connector in the dimeric enzyme and that this catalytic site is independent of the cleavage status in the second connector.

Processing of Endogenous Executioner Caspases

We next analyzed whether single cleavage of caspase-7 occurs with the endogenous protein in cytosolic extracts. The experiments rely on the capture of active caspases by biotinyl-hex-EVD-acyloxymethyl ketone (bEVD-AOMK) (Kato et al., 2005), which under nondenaturing conditions should allow simultaneous capture of the unprocessed (unlabeled) catalytic unit in a partially processed heterodimer.

We obtained hypotonic extracts of human 293A cells that are capable of supporting a cell-free apoptotic pathway (Ellerby et al., 1997; Li et al., 1997). Caspase activation was initiated by addition of cytochrome c (cyt c) and dATP followed by the addition of bEVD-AOMK (Figure 5A). The ABP was allowed to incubate for 30 min to label caspase active sites, and reactive proteins were captured by using immobilized streptavidin. To maximize the probability of capturing such molecules, we optimized the conditions (stimulus and time) so robust processing is obtained but plenty of zymogen is left. Analysis revealed processing of caspase-7 and -3 (Figure 5A, left), and almost all ABP bound to the large subunits (Figure 5A, right). We were able to identify a small amount of single chain caspase-7 at early time points that we estimate at less than 5% of the detected protein. These results reveal that single cleavage of procaspase-7 dimers occurs during apoptosome formation in cytosolic extracts but that the majority of procaspase-7 is efficiently cleaved at both interchain connectors. Notably, no single chain form of caspase-3 was captured.

Our results predict that singly cleaved and active executioner caspase dimers could exist in cells. To test this prediction, we proposed that if such a dimer exists, we should be able to detect it by using the above approach. We thus developed a cell-permeable version of bEVD-AOMK that we characterized (see Supplemental Experimental Procedures and Figure S5).

Jurkat T cells were labeled for 1 hr with 1 μM O-methylated bEVD-AOMK after 1 or 2 hr of treatment with αFas antibodies. Those time points provide good detectable activation, but most of the zymogen remains to maximize our chances of detecting singly cleaved molecules. The proteasome inhibitor MG-132 was used to prevent removal of caspase-3 during extrinsic pathway stimulation (Tawa et al., 2004). Lysates were prepared with protease inhibitors (see Experimental Procedures) and subjected to capture of labeled proteins with streptavidin beads (Figure 5B). Immunoblotting with anti-caspase-7 and -3 antibodies failed to detect any single chain caspase despite the strong detection of the large subunits of cleaved caspase-7 and -3 (lanes 1 and 2, Figure 5B, right). Those findings reveal that the DISC and the apoptosome are very efficient at processing executioner caspase zymogens.

Discussion

Assembly of the Caspase-7 Zymogen

Active forms of caspases are obligate dimers, with the dimer interface providing important contacts that stabilize the catalytic conformation. Initial structural studies of active caspases suggested a domain-swapping model where the zymogen was formed by interdigitation of the C-terminal subdomain of each monomer to generate a tightly associated dimer (Wei et al., 2000; Wilson et al., 1994). The alternative possibility is that the zymogen dimer forms by simple association, and it was expected that structures of the zymogen form of caspase-7 would be able to settle this issue (Chai et al., 2001; Riedl et al., 2001). However, lack of crystallographic detail in the connector failed to deliver resolution. Using our differentially tagged caspase-7 constructs, we demonstrate that the interdigitation model is incorrect for recombinant material in *E. coli*, and we see no reason to postulate otherwise for human cells in vivo. Thus, the zymogen of caspase-7 forms by direct association of the C-terminal region of the catalytic domains. Our results do not exclude that the dimers of the other executioner caspases-3 and -6 form through interdigitation, but based on (1) the high amino acid identity between caspase-7 and caspase-3 or -6 catalytic domain (57% and 42%, respectively), (2) almost identical residues found at the dimer interface, and (3) conservation of mechanism within a protein family, we infer that they most likely behave similarly. In contrast to the executioner caspases, the zymogens of initiator caspases such as caspase-8 and -9 are monomeric, and activation occurs after dimerization. Consequently, the formation of active initiator caspases and zymogen executioner caspases is likely to follow the same assembly pathway—simple association of prefolded monomeric catalytic domains without domain swapping. This is supported by the observation that dissociation of caspase-3 dimers proceeds much more readily than dissociation of the individual units of a catalytic domain (Bose and Clark, 2001). To our knowledge, our findings constitute the first unequivocal demonstration that an executioner caspase dimer is formed through direct dimerization.

Mobility in the Caspase-7 Zymogen

Cleavage in the interchain connector is necessary and sufficient for the activation of procasapse-7 (Chai et al., 2001; Zhou and Salvesen, 1997). Substantial discussion in the literature has focused on the importance of a four-strand bundle that locks down the active site of caspase-7 into its catalytic conformation (Chai et al., 2001; Fuentes-Prior and Salvesen, 2004; Riedl et al., 2001; Riedl and Shi, 2004), with the general assumption

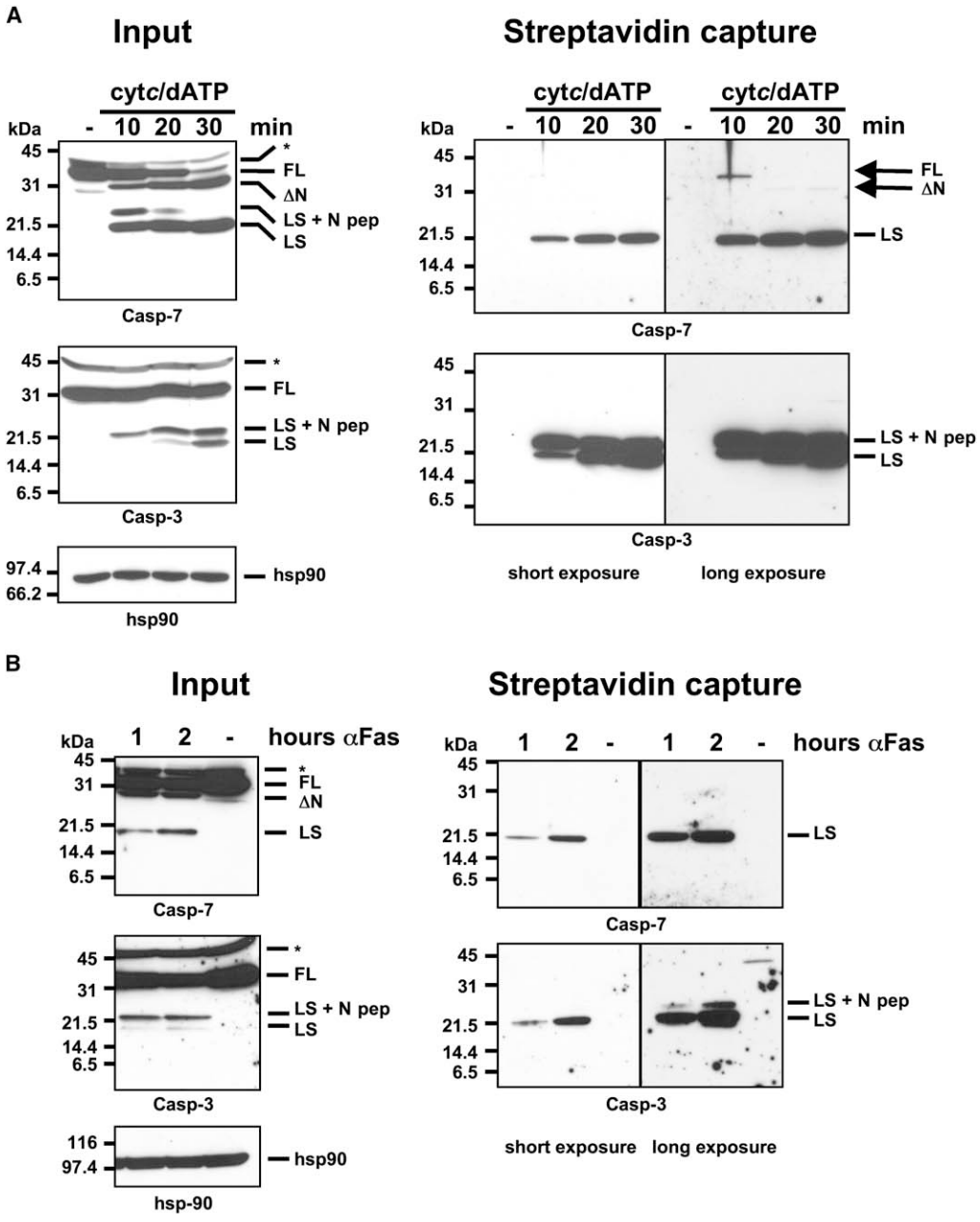

Figure 5. The Apoptosome and the DISC Efficiently Process Executioner Caspases

(A) A hypotonic extract from 293A cells was activated with cyt c (10 μM) and dATP (1 mM) for the indicated period of time before addition of 10 μM bEVD-AOMK for 30 min. Input samples (left) and affinity-captured samples (right) were analyzed by immunoblotting with antibodies specific to caspase-7, caspase-3, and hsp90. Short film exposure (2 min) and long exposure (30 min) of precipitated proteins are presented. Importantly, note the full-length caspase-7 band captured by streptavidin and observed in the long exposure (arrows). The asterisks mark nonspecific cross-reactive proteins detected by the antibody used.

(B) Jurkat cells were treated with anti-Fas antibodies in the presence of MG-132 for the indicated period of time followed by incubation with (OMe)bEVD-AOMK. Lysate and streptavidin-captured proteins were analyzed as in (A). Unprocessed executioner caspases are not observed in the captured samples visualized either by short film exposure (2 min) or long exposure (30 min). ΔN, full-length protein lacking the N peptide; FL, full-length; LS, large subunit; and N pep, N peptide.

that both interchain connectors of the zymogen must be cleaved for this to occur (doubly cleaved zymogen). We show that this assumption is false and that only one of the connectors must be cleaved (singly cleaved zymogen). The singly cleaved zymogen displays half the catalytic rate of fully cleaved dimer, because it only has one active site. However, the catalytic efficiency of that site is indistinguishable from the catalytic efficiency of one site of a fully cleaved dimer. This unexpected result at first glance seems to negate the importance of the four-strand bundle in catalytic activity, because the crystal structures should not allow for such a structure. However, evidence for the importance of the bundle structure comes from our results of mutagenesis of

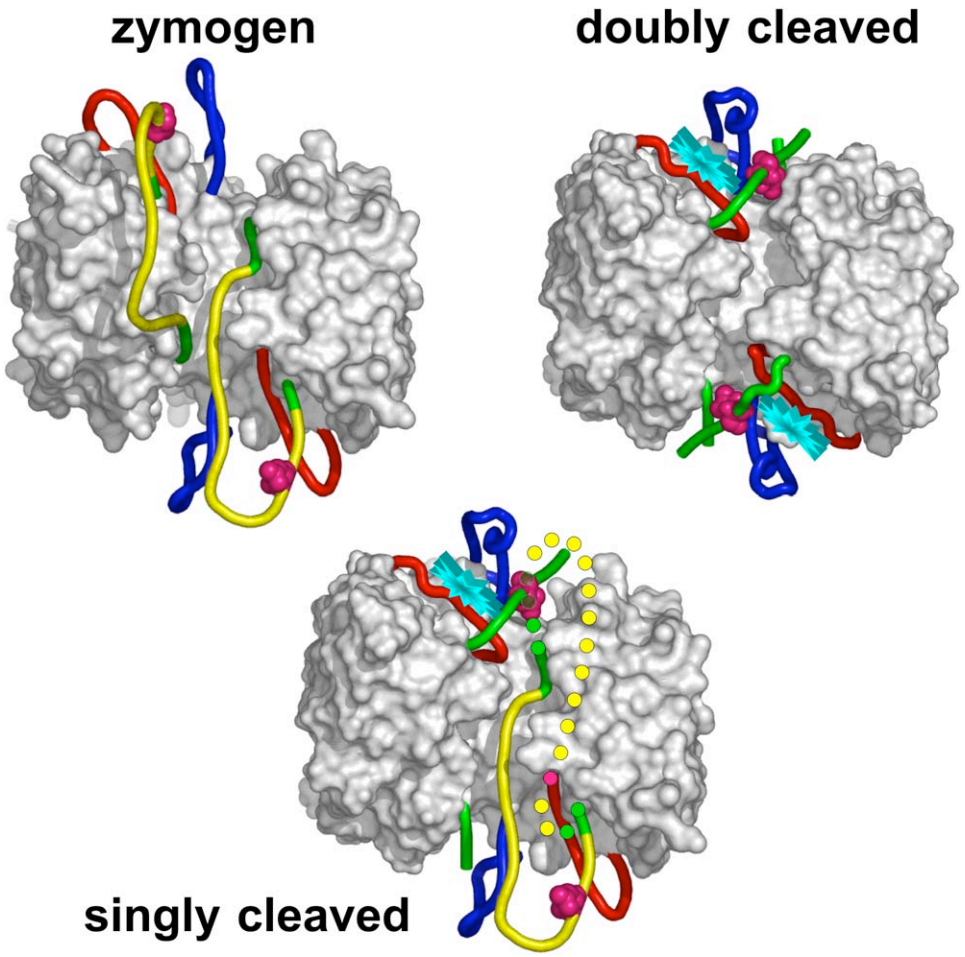

Figure 6. Model for the Singly Cleaved Dimer

Catalytic units from the zymogen (PDB 1GQF; Riedl et al., 2001) and the doubly cleaved form (PDB 1F1J; Wei et al., 2000) were combined to generate the singly cleaved caspase-7 model. This theoretical model is used to visualize the possible movements of the interchain connector. Conserved structural regions between the zymogen and doubly cleaved crystal structures are shown in surface representation. Red and blue loops carry determinants of the catalytic and specificity apparatus, the green/yellow loop is the interdomain connector, the cyan star represents the active site, and the magenta balls designate Asp192. In the zymogen and the singly cleaved models, the portion of the interdomain connector that lacks defined electron density in the zymogen crystal structure is colored yellow. In the singly cleaved form, interactions with Asp192 and formation of the associated loop bundle are allowed by movement of the uncleaved connector (circles). This movement precludes formation of the second loop bundle, and cleavage of the connector is required to relieve the constraints and allow full maturation of the second catalytic site.

Asp192. This residue, which is conserved in caspase-2, -3, -6, -7, -9, and -14, forms critical contacts with the neighboring N-terminal stalk of the adjacent cleaved catalytic domain of the dimer (Chai et al., 2001). Consequently, any model of singly cleaved caspase-7 must account for preserving the Asp192 interaction with the adjacent connector. It is possible to model this structure without violating structural constraints by repositioning the connector of the uncleaved unit, as diagrammed in Figure 6. This model is allowed given the notable mobility of the inter-chain connector.

The crystal structures of procaspase-7 show no reliable electron density for most of the residue that constitute the connector. This fits well with a critical requirement for proteolysis of native proteins: that cleavage sites be in nonstructured regions (Hubbard et al., 1991). Formation of the first catalytic site of a dimer after the initial cleavage will cause ordering of the loop bundle. This should diminish movement of the other, yet uncleaved, connector. Indeed, one would expect the uncleaved connector to occupy the central cavity at the dimer interface (Riedl et al., 2001). Hardy and colleagues have shown that the central cavity at the dimer interface is accessible to the small thiol-reactive compound 2-(2,4-Dichlorophenoxy)-N-(2-mercapto-ethyl)-acetamide (DICA) (Hardy et al., 2004). We reasoned that the singly cleaved dimer should be inaccessible to DICA if the uncleaved connector occupies the central cavity. In experiments not shown here, we found that DICA was able to label uncleaved, singly cleaved, and doubly cleaved caspase-7, demonstrating that the central cavity is not substantially blocked by the uncleaved connector.

Despite the flexibility of the caspase-7 interchain connector, at least one cleavage is required to form one active site. Contrast this with the apical caspase-8 and -9, which require no cleavage for generation of activity. This is probably due to the much longer interchain connectors of the apical caspases, which allow for loop bundle

formation without cleavage. Indeed, the flexibility and extended length of the interchain connector partly explain the key distinction between apical and executioner caspases. Our model does not exclude that the uncleaved domain of a singly cleaved dimer may attain some activity, or even a slightly altered specificity, especially given the evident mobility of the interchain connector. Indeed, Berger and colleagues have identified such an intermediate by using a new generation of selective ABPs and show evidence that this singly cleaved caspase-7 has a distinct substrate specificity (Berger et al., 2006).

A Mechanism for Optimization of Apical Caspase Activity

The two active sites of initiator caspase-8 can be docked, at least in silico, onto the general space occupied by the modeled interchain connector region of procaspase-7. This suggested a possible cooperative mechanism of cleavage and activation of caspase-7, where both connectors were simultaneously cleaved. However, activation by caspase-8 as a dimer or as a heterodimer with FLIP in vitro demonstrated no obvious cooperativity. Furthermore, the crystal structure of caspase-9 (Renatus et al., 2001) shows only one active site within the dimer, excluding the possibility for a cooperativity mechanism for caspase-9. This implies that each connector has an independent opportunity to be cleaved by caspase-8, and therefore, we expected to be able to detect singly cleaved caspase-3 and -7 dimers in more physiologic settings. Although we were able to detect singly cleaved caspase-7 in cytosolic extracts programmed by the natural activation of caspase-9, we were unable to detect any in cells triggered by conventional apoptotic signals. This signifies that the activation of caspase-3 and -7 in vivo may be a very efficient event and that both interchain connectors are cleaved in the apical activation complexes that employ caspase-8 and -9, before the caspase leaves the activation assembly.

Procaspase-7 activation assays performed in low-salt buffer gave ~10-fold higher activation rates than in high salt (Table 1), and this may be due to the greater viscosity of the high-salt buffer. Notwithstanding this, the inherent activity of recombinant initiator caspases-8 and -9 against procaspase-7, measured as a function of k_{cat}/K_M, in either low-salt or high-salt buffer is substantially less than the activity of GrB on the procaspase. The difference between these two types of proteolytic activator in vivo is that GrB is delivered to target cells in a readily diffusible form, whereas apical caspase activation requires assembly of zymogens in multimeric complexes. We propose that an additional important function of the multimeric apical caspase activation platforms, the DISC (caspase-8 and -10 activator) and the apoptosome (caspase-9 activator), is to increase the functional efficiency of the initiator caspase cleavage rates. Thus, the local availability of multiple apical caspase active sites increases the likelihood of complete procaspase-7 activation in vivo, overcoming the less than optimal inherent catalytic efficiencies of the single molecules. A logical consequence of this proposal is that apical caspase activity should be mainly confined to the multimeric complexes. Indeed, this is supported by studies showing that Fas forms large aggregates upon stimulation (Kischkel et al., 1995) and that cells treated with anti-Fas antibody show highly localized cleaved caspase-8 immunostaining surrounding internalized Fas (Lee et al., 2006). Gel filtration analysis demonstrates that caspase-9 activity is restricted to the high molecular weight apoptosome-containing fractions (Cain et al., 1999), with no activity in the lower molecular weight caspase-9-containing material. Therefore, not only is activation of apical caspase zymogens facilitated by concentration in the DISC or apoptosome but also the efficiency of the activated apical caspases is enhanced in vivo by local high concentration in these assemblies.

The enhancement of apical caspase activity in vivo appears distinct from the optimization of catalytic efficiency in other signaling events, such as the MAPK and ERK protein kinases (Kolch, 2005) and NFκB (Hayden and Ghosh, 2004) pathways, and the proteolytic activation pathway of blood coagulation (Ahmad et al., 2003). In these cases, efficiency is optimized, and the flux of information is passed, by template-driven recruitment of substrates to enzymes either via protein scaffolds, or by association of cofactors to biological membranes. In contrast, the apoptotic pathways that converge on caspase-3 and -7 activation appear not to require recruitment of substrates. They rely on a strategy for activation of apical caspases within multimeric activation complexes yet allow simple diffusion in and out of their target substrates, the executioner caspase zymogens. This strategy is enhanced by the high mobility of the sensitive cleavage sites of the executioner zymogens.

Experimental Procedures

Cell Lines and Tissue Culture

Jurkat cells (E6-1) were cultured in RPMI medium supplemented with 10% fetal bovine serum, 2 mM L-glutamine, and antibiotics and maintained at $0.1 - 2 \times 10^6$ cells/ml. 293A cells (QBI-hEK-293A/293-Ad, Q-Biogene, Irvine CA) were grown in DME medium supplemented as above.

Plasmids and Recombinant Proteins

Human caspase-7 cDNA (GenBank accession number NM_001227) was used for all constructs. Site-directed mutagenesis was done with the QuikChange XL method (Stratagene, Cedar Creek, TX) or overlapping PCR. Caspase-7 cDNA was subcloned into pET-23b(+) (Novagen, Madison, WI) in the NdeI-XhoI sites to yield C-terminal His-tagged protein. Alternatively, PCR was used to amplify caspase-7 with a T7 oligonucleotide and an oligonucleotide adding a Flag epitope to the C terminus (5′-GGGCTCGAGCTACTTGTCA TCGTCGTCCTTGTAGTCTTGACTGAAGTAGAGTTCC-3′) and subcloned into NdeI-XhoI sites of pET-28b(+). Recombinant expression constructs for ΔDEDs-caspase-8 (Casp-8) (Boatright et al., 2003), ΔCARD-caspase-9 (Casp-9) (Renatus et al., 2001), ΔDEDs-caspase-10 (Casp-10), and ΔDEDs-FLIPL (FLIP) (Boatright et al., 2004) constructs were previously described. Expression construct for ΔCARD-caspase-2 comprises residues 160–434 of human caspase-2 (GenBank accession number AAP35904) subcloned into the NdeI and XhoI sites of pET-23b(+) and expressed as described for caspase-3 (Stennicke and Salvesen, 1999). Proteins were expressed in the presence of pLysS and purified as previously described (Stennicke and Salvesen, 1999). Procaspase-7 zymogen proteins were obtained by using 0.2 mM isopropyl-β-D-thiogalactopyranoside (IPTG) for 0.5–1 hr, whereas mature proteins were obtained within 6–8 hr. With the exception of caspase-9, each active caspases was active-site titrated with the irreversible caspase

inhibitor zVAD-FMK as described (Stennicke and Salvesen, 2000). The baculovirus caspase inhibitor p35 (Zhou and Salvesen, 2000) was used to titrate caspases whenever zVAD-FMK titration was ineffective.

Caspase-7 hybrid dimers were produced as above in media containing ampicillin (50 μg/ml), kanamycin (25 μg/ml), and chloramphenicol (25 μg/ml) and induced with 0.2 mM IPTG for 0.5 or 6 hr. Proteins were purified by Ni^{2+}-affinity chromatography as previously described (Stennicke and Salvesen, 1999). The eluate (in low-salt buffer [50 mM Tris (pH 7.4), 100 mM NaCl] containing 50–150 mM imidazole) was mixed with 1–2 ml of M2-Affigel (Sigma-Aldrich) and incubated for 2 hr at 4°C with rocking. Resin was collected by centrifugation, washed three times with ten volumes of 0.5 M NaCl in 50 mM Tris (pH 7.4) and poured in a disposable column. The column was further washed with ten bed volumes of low-salt buffer, and proteins were eluted with 7 ml of 100 μg/ml Flag peptide in the same buffer. With the exception of the active heterodimers produced to demonstrate the feasibility of the sequential purification, all heterodimers were expressed for short periods (0.5 hr) to prevent overrepresentation of one form over another. Because Flag-tagged caspase-7 sticks to the Ni^{2+} resin, some Flag-tagged homodimer is present after the second purification step. This was remedied by a second Ni^{2+} resin purification, extensive washing of the beads, and imidazole step elution.

Caspase Assays

Due to propensity of caspase-7 to precipitate in various assay conditions, assays must be performed quickly and handling of the protein should be minimized. Assays were performed at 37°C in a volume of 100 μl containing substrate and hydrolysis rates determined with a Molecular Device spectrophotometer (abs 405 nm) or fMAX fluorometer (excitation 405 nm, emission 510 nm) plate readers operating in the kinetic mode. Kinetic parameters were determined in standard caspase buffer (10 mM PIPES [pH 7.2], 100 mM NaCl, 10% sucrose, 0.1% CHAPS, 10 mM DTT, and 1 mM EDTA), low-salt (100 mM HEPES [pH 7.0], 50 mM NaCl, 0.01% CHAPS, and 10 mM DTT), or high-salt (low-salt buffer containing 1M sodium citrate) buffer as indicated.

Activation assays with GrB and initiator caspases were performed essentially as described elsewhere (Zhou and Salvesen, 1997; Stennicke et al., 1998). The detailed procedure is reproduced in the Supplemental Experimental Procedures.

SDS-PAGE and Immunoblots

Proteins were routinely analyzed on 2-amino-2-methyl-1,3-propanediol gradient SDS-PAGE (Bury, 1981) and blotted on PVDF membrane in 10 mM CAPS [pH 11] and 10% methanol. Proteins from lysates were loaded based on initial cell number to reflect for protein lost due to apoptosis. For immunoblot quantification, proteins were resolved on 10%/12% uniform SDS-PAGE, blotted, and analyzed by using monoclonal anti-caspase-7 antibody. Signal quantification was performed by using a CCD camera on exposing blots and analyzed on imaging software ChemImager 4000.

Caspase Labeling Using ABP

Jurkat cells were harvested at 1×10^6 cells/ml, resuspended in fresh media at 2×10^6 cells ml^{-1} containing 200 ng/ml anti-Fas CH-11 antibodies for the indicated period of time; most samples were composed of 1×10^7–3×10^7 cells. For in vivo labeling, cells were harvested and incubated in fresh media at 5×10^7 cells/ml in the presence of 10 μM O-methylated bEVD-AOMK for 1 hr. Cells were washed twice in cold PBS and extracts were prepared in lysis buffer (50 mM Tris [pH 7.4], 100 mM NaCl, 1% NP-40, 0.5% deoxycholic acid, and 1 mM EDTA) containing protease inhibitors (1 mM 1,10-orthophenanthroline, 10 μM E-64, 10 μM 3,4-dichloroisocoumarin, 10 μM leupeptin, and 1 μM MG-132) and caspase inhibitors (100 μM zVAD-FMK and 100 μM AcDEVD-CHO). At the indicated concentration, none of the general protease inhibitor used has a significant effect on the activity of caspase-3 or -7 in a standardized assay, whereas zVAD-FMK and AcDEVD-CHO completely abolish caspase activity.

In vitro labeling in hypotonic extract was carried out as follows. 293A cell hypotonic extract was prepared as described (Deveraux et al., 1997). A typical assay consists of a 50 μl reaction containing 100–200 μg of proteins. Caspase activation was triggered by the addition of 10 μM horse cyt c (Sigma-Aldrich) and 1 mM dATP and incubation at 37°C for the indicated period of time. Extracts were then incubated for 30 min with 1 μM bEVD-AOMK at 37°C. General protease and caspase inhibitors were added after the labeling period.

An aliquot of each sample was kept for input immunoblots. All samples were completed to 0.5 ml in pull-down buffer (50 mM Tris [pH 7.4], 100 mM NaCl, 1% IGEPAL, and 0.5% deoxycholic acid) containing all protease inhibitors. Biotinylated proteins were precipitated with 25 μl of streptavidin beads per 1×10^7 cells or per hypotonic extract sample. Beads were washed once with pull-down buffer and three times with PBS. Proteins were eluted by boiling in one bead volume of SDS-PAGE buffer containing 1 mM d-biotin.

Recombinant caspases were labeled with the indicated concentration of ABP in standard or high-salt buffer (see above) for 30 min at 37°C. Reactions were stopped by boiling samples in SDS-PAGE loading buffer containing 1 mM d-biotin and analyzed by using streptavidin-HRP. Alternatively, enough streptavidin beads were added to bind twice the molar amount of ABP, and biotinylated proteins were analyzed as described above.

Supplemental Data

Supplemental Data include Supplemental Experimental Procedures, Supplemental References, five figures, and two tables and can be found with this article online at http://www.molecule.org/cgi/content/full/23/4/523/DC1/.

Acknowledgments

We thank Scott J. Snipas and AnneMarie Price for outstanding technical assistance, Henning Stennicke for advice, Constantina Bakolitsa for modeling, and Eric Wildfang for MALDI analysis. This work is supported by National Institutes of Health grants NS37878 to G.S.S. and RR20843 to G.S.S. and M.B.

Received: April 3, 2006
Revised: May 19, 2006
Accepted: June 7, 2006
Published: August 17, 2006

References

Ahmad, S.S., London, F.S., and Walsh, P.N. (2003). The assembly of the factor X-activating complex on activated human platelets. J. Thromb. Haemost. *1*, 48–59.

Berger, A.B., Witte, M.D., Denault, J.-B., Sadaghiani, A.M., Sexton, K.M.B., Salvesen, G.S., and Bogyo, M. (2006). Identification of early intermediates of caspase activation using selective inhibitors and activity-based probes. Mol. Cell *23*, this issue, 509–521.

Boatright, K.M., and Salvesen, G.S. (2003). Mechanisms of caspase activation. Curr. Opin. Cell Biol. *15*, 725–731.

Boatright, K.M., Renatus, M., Scott, F.L., Sperandio, S., Shin, H., Pedersen, I., Ricci, J.-E., Edris, W.A., Sutherlin, D.P., Green, D.R., and Salvesen, G.S. (2003). A unified model for apical caspase activation. Mol. Cell *11*, 529–541.

Boatright, K.M., Deis, C., Denault, J.B., Sutherlin, D.P., and Salvesen, G.S. (2004). Activation of caspases 8 and 10 by FLIP L. Biochem. J. *382*, 651–657.

Bose, K., and Clark, A.C. (2001). Dimeric procaspase-3 unfolds via a four-state equilibrium process. Biochemistry *40*, 14236–14242.

Bury, A. (1981). Analysis of protein and peptide mixtures: Evaluationof three sodium dodecyl sulphate-polyacrylamide gel electrophoresis buffer systems. J Chromatog *213*, 491–500.

Cain, K., Brown, D.G., Langlais, C., and Cohen, G.M. (1999). Caspase activation involves the formation of the aposome, a large (approximately 700 kDa) caspase-activating complex. J. Biol. Chem. *274*, 22686–22692.

Chai, J., Wu, Q., Shiozaki, E., Srinivasula, S.M., Alnemri, E.S., and Shi, Y. (2001). Crystal structure of a procaspase-7 zymogen. Mechanisms of activation and substrate binding. Cell *107*, 399–407.

Denault, J.B., and Salvesen, G.S. (2002). Caspases: keys in the ignition of cell death. Chem. Rev. *102*, 4489–4500.

Denault, J.B., and Salvesen, G.S. (2003). Human caspase-7 activity and regulation by its N-terminal peptide. J. Biol. Chem. *278*, 34042–34050.

Deveraux, Q., Takahashi, R., Salvesen, G.S., and Reed, J.C. (1997). X-linked IAP is a direct inhibitor of cell death proteases. Nature *388*, 300–304.

Ellerby, H.M., Martin, S.J., Ellerby, L.M., Naiem, S.S., Rabizadeh, S., Salvesen, G.S., Casiano, C.A., Cashman, N.R., Green, D.R., and Bredesen, D.E. (1997). Establishment of a cell-free system of neuronal apoptosis: comparison of premitochondrial, mitochondrial, and postmitochondrial phases. J. Neurosci. *17*, 6165–6178.

Fischer, U., Janicke, R.U., and Schulze-Osthoff, K. (2003). Many cuts to ruin: a comprehensive update of caspase substrates. Cell Death Differ. *10*, 76–100.

Fuentes-Prior, P., and Salvesen, G.S. (2004). The protein structures that shape caspase activity, specificity, activation and inhibition. Biochem. J. *384*, 201–232.

Green, D.R., and Evan, G.I. (2002). A matter of life and death. Cancer Cell *1*, 19–30.

Gu, Y., Wu, J.W., Faucheu, C., Lalanne, J.L., Diu, A., Livingston, D.J., and Su, M.S.S. (1995). Interleukin-1-beta converting enzyme requires oligomerization for activity of processed forms in vivo. EMBO J. *14*, 1923–1931.

Hardy, J.A., Lam, J., Nguyen, J.T., O'Brien, T., and Wells, J.A. (2004). Discovery of an allosteric site in the caspases. Proc. Natl. Acad. Sci. USA *101*, 12461–12466.

Hayden, M.S., and Ghosh, S. (2004). Signaling to NF-kappaB. Genes Dev. *18*, 2195–2224.

Hubbard, S.J., Campbell, S.F., and Thornton, J.M. (1991). Molecular recognition. Conformational analysis of limited proteolytic sites and serine proteinase protein inhibitors. J. Mol. Biol. *220*, 507–530.

Kato, D., Boatright, K.M., Berger, A.B., Nazif, T., Blum, G., Ryan, C., Chehade, K.A.H., Salvesen, G.S., and Bogyo, M. (2005). Activity-based probes that target diverse cysteine protease families. Nat. Chem. Biol. *1*, 33–38.

Kischkel, F.C., Hellbardt, S., Behrmann, I., Germer, M., Pawlita, M., Krammer, P.H., and Peter, M.E. (1995). Cytotoxicity-dependent APO-1 (Fas/CD95)-associated proteins form a death-inducing signaling complex (DISC) with the receptor. EMBO J. *14*, 5579–5588.

Kolch, W. (2005). Coordinating ERK/MAPK signalling through scaffolds and inhibitors. Nat. Rev. Mol. Cell Biol. *6*, 827–837.

Lee, K.H., Feig, C., Tchikov, V., Schickel, R., Hallas, C., Schutze, S., Peter, M.E., and Chan, A.C. (2006). The role of receptor internalization in CD95 signaling. EMBO J. *25*, 1009–1023.

Li, P., Nijhawan, D., Budihardjo, I., Srinivasula, S.M., Ahmad, M., Alnemri, E.S., and Wang, X. (1997). Cytochrome c and dATP-dependent formation of Apaf-1/caspase-9 complex initiates an apoptotic protease cascade. Cell *91*, 479–489.

Pop, C., Chen, Y.-R., Smith, B., Bose, K., Bobay, B., Tripathy, A., Franzen, S., and Clark, C. (2001). Removal of the pro-domain does not affect the conformation of the procaspase-3 dimer. Biochemistry *40*, 14224–14235.

Renatus, M., Stennicke, H.R., Scott, F.L., Liddington, R.C., and Salvesen, G.S. (2001). Dimer formation drives the activation of the cell death protease caspase 9. Proc. Natl. Acad. Sci. USA *98*, 14250–14255.

Riedl, S.J., and Shi, Y. (2004). Molecular mechanisms of caspase regulation during apoptosis. Nat. Rev. Mol. Cell Biol. *5*, 897–907.

Riedl, S.J., Fuentes-Prior, P., Renatus, M., Kairies, N., Krapp, R., Huber, R., Salvesen, G.S., and Bode, W. (2001). Structural basis for the activation of human procaspase-7. Proc. Natl. Acad. Sci. USA *98*, 14790–14795.

Roy, S., Bayly, C.I., Gareau, Y., Houtzager, V.M., Kargman, S., Keen, S.L., Rowland, K., Seiden, I.M., Thornberry, N.A., and Nicholson, D.W. (2001). Maintenance of caspase-3 proenzyme dormancy by an intrinsic "safety catch" regulatory tripeptide. Proc. Natl. Acad. Sci. USA *98*, 6132–6137.

Scott, F.L., Denault, J.B., Riedl, S.J., Shin, H., Renatus, M., and Salvesen, G.S. (2005). XIAP inhibits caspase-3 and -7 using two binding sites: evolutionarily conserved mechanism of IAPs. EMBO J. *24*, 645–655.

Stennicke, H.R., and Salvesen, G.S. (1999). Caspases: preparation and characterization. Methods *17*, 313–319.

Stennicke, H.R., and Salvesen, G.S. (2000). Caspase assays. Methods Enzymol. *322*, 91–100.

Stennicke, H.R., Jurgensmeier, J.M., Shin, H., Deveraux, Q., Wolf, B.B., Yang, X., Zhou, Q., Ellerby, H.M., Ellerby, L.M., Bredesen, D., et al. (1998). Pro-caspase-3 is a major physiologic target of caspase-8. J. Biol. Chem. *273*, 27084–27090.

Tawa, P., Hell, K., Giroux, A., Grimm, E., Han, Y., Nicholson, D.W., and Xanthoudakis, S. (2004). Catalytic activity of caspase-3 is required for its degradation: stabilization of the active complex by synthetic inhibitors. Cell Death Differ. *11*, 439–447.

Wei, Y., Fox, T., Chambers, S.P., Sintchak, J., Coll, J.T., Golec, J.M., Swenson, L., Wilson, K.P., and Charifson, P.S. (2000). The structures of caspases-1, -3, -7 and -8 reveal the basis for substrate and inhibitor selectivity. Chem. Biol. *7*, 423–432.

Wilson, K.P., Black, J.A., Thomson, J.A., Kim, E.E., Griffith, J.P., Navia, M.A., Murcko, M.A., Chambers, S.P., Aldape, R.A., Raybuck, S.A., and Livingston, D.J. (1994). Structure and mechanism of interleukin-1 beta converting enzyme. Nature *370*, 270–275.

Zhou, Q., and Salvesen, G.S. (1997). Activation of pro-caspase-7 by serine proteases includes a non-canonical specificity. Biochem. J. *324*, 361–364.

Zhou, Q., and Salvesen, G.S. (2000). Viral caspase inhibitors CrmA and p35. Methods Enzymol. *322*, 143–154.